



3 4456 0604296 6

K/CSD/TM-63
Dist. Category: UC-22

MARTIN MARIETTA

**A FINITE VOLUME SCHEME FOR CALCULATING
THE INTERIOR FLOW IN A GAS CENTRIFUGE**

John R. Kirkpatrick

December 1986

This document has been reviewed for Unclassified-Sensitive issues. The review resulted in a decision the document is void of U-S issues and that the 3/18/1987 ETPP CICO public release approval is not valid.
G. A. McBride/dw 3/28/2011
BJC ETPP Classification and Information Control Office

~~K25RC~~

This document is approved for public release per review by:

A. S. Quist/dw 3/18/1987
K-25 Classification & Information Date
Control Office

OPERATED BY
MARTIN MARIETTA ENERGY SYSTEMS, INC.
FOR THE UNITED STATES
DEPARTMENT OF ENERGY

Printed in the United States of America. Available from
National Technical Information Service
U.S. Department of Commerce
5285 Port Royal Road, Springfield, Virginia 22161
NTIS price codes—Printed Copy: A03 Microfiche A01

This report was prepared as an account of work sponsored by an agency of the United States Government. Neither the United States Government nor any agency thereof, nor any of their employees, makes any warranty, express or implied, or assumes any legal liability or responsibility for the accuracy, completeness, or usefulness of any information, apparatus, product, or process disclosed, or represents that its use would not infringe privately owned rights. Reference herein to any specific commercial product, process, or service by trade name, trademark, manufacturer, or otherwise, does not necessarily constitute or imply its endorsement, recommendation, or favoring by the United States Government or any agency thereof. The views and opinions of authors expressed herein do not necessarily state or reflect those of the United States Government or any agency thereof.

Dist. Category: UC-22,
Isotope Separation

K/CSD/TM-63

A FINITE VOLUME SCHEME FOR CALCULATING
THE INTERIOR FLOW IN A
GAS CENTRIFUGE

John R. Kirkpatrick

December 1986

Computing and Telecommunications Division
at
Oak Ridge Gaseous Diffusion Plant
Post Office Box P
Oak Ridge, Tennessee 37831

MARTIN MARIETTA ENERGY SYSTEMS, INC.
operating the
Oak Ridge Gaseous Diffusion Plant . . . Oak Ridge National Laboratory
Oak Ridge Y-12 Plant . . . Paducah Gaseous Diffusion Plant
Under Contract No. DE-AC05-84OR21400
for the
U.S. DEPARTMENT OF ENERGY

By acceptance of this article,
the publisher or recipient
acknowledges the U.S. Govern-
ment's right to retain a non-
exclusive, royalty-free license
in and to any copyright
covering the article.



CONTENTS

	<u>Page</u>
ABSTRACT	1
1. INTRODUCTION	3
2. ASSUMPTIONS	5
3. EQUATIONS OF MOTION	7
4. FINITE VOLUME EQUATIONS AND SOLUTION METHODS	11
4.1 RADIAL MOMENTUM	14
4.2 AXIAL MOMENTUM	17
4.3 CONTINUITY (PRESSURE)	18
4.4 ANGULAR MOMENTUM	21
4.5 ENERGY	23
4.6 SOURCE AND SINK TERMS	26
4.7 ORDER OF EQUATIONS IN SOLUTION	27
5. STABILITY AND LIMITATIONS OF THE METHOD	29
6. RESULTS	31
ACKNOWLEDGMENTS	35
REFERENCES	37

ABSTRACT

A numerical algorithm which is designed to calculate the flow patterns in a gas centrifuge is presented. The nodal equations are derived using finite volume concepts, thus ensuring rigorous conservation of mass, momentum, and energy for the computational cells and for the entire rotor. The method for solving the systems of nodal equations is designed to produce a steady-state solution using a mixture of time-dependent and time-independent equations. Streamlines for a sample configuration are shown. Comparison with results published by other authors shows good agreement.

1. INTRODUCTION

The gas centrifuge has come into prominence as a potential tool for enriching uranium for use in nuclear reactors (refs. 1-3). Britain, West Germany, and the Netherlands have plants in operation. Japan is building a plant, while the United States has cancelled further construction on its partially completed plant. The desire to build centrifuges brings with it a need to calculate their performance. There have been many papers published on aspects of centrifuge calculation. Workshops on "Gases in Strong Rotation" have been held on a biannual basis since 1975.

Figure 1.1 shows a schematic of a typical gas centrifuge. Olander's article (ref. 1) contains a detailed description of the configuration and an explanation of its operation. The separation chamber itself contains only a few crucial features. Near the bottom is a stationary scoop which draws off the tails flow. The top of the chamber is a baffle with holes in it through which the product flow is drawn into an upper chamber where it is picked up by another scoop. The feed material is introduced at the axis. In addition to the dimensions and rotational speed of the chamber, the locations of the tails scoop, product holes, and feed point; the flows through these features; the drag on the tails scoop; a measure of the mass of gas contained within the chamber; and the temperatures of the rotor wall (and perhaps the end caps) form a sufficient set of data to be able to calculate the flow within the chamber and thus its separative performance.

In 1974, James A. Viecelli (ref. 3) of the Lawrence Livermore National Laboratory (LLNL) proposed a set of equations which he believed would be sufficient to describe the flow in a centrifuge. He made approximations to the Navier-Stokes equations of a boundary layer nature drawing on estimates and preliminary calculations done by others who had studied the problem as well as the usual boundary layer arguments. He then assembled a finite difference algorithm for his equations and a solution scheme for the resulting set of node equations. Viecelli's scheme was adopted by J. E. Park of Martin Marietta Energy Systems, Inc., who modified some boundary conditions and changed the difference algorithm for the energy equation. The present author took over from Park and has continued the evolution of the scheme. Neither Viecelli nor Park has published any of his work on this. The author will make an effort to show which of the ideas to be presented here are theirs.

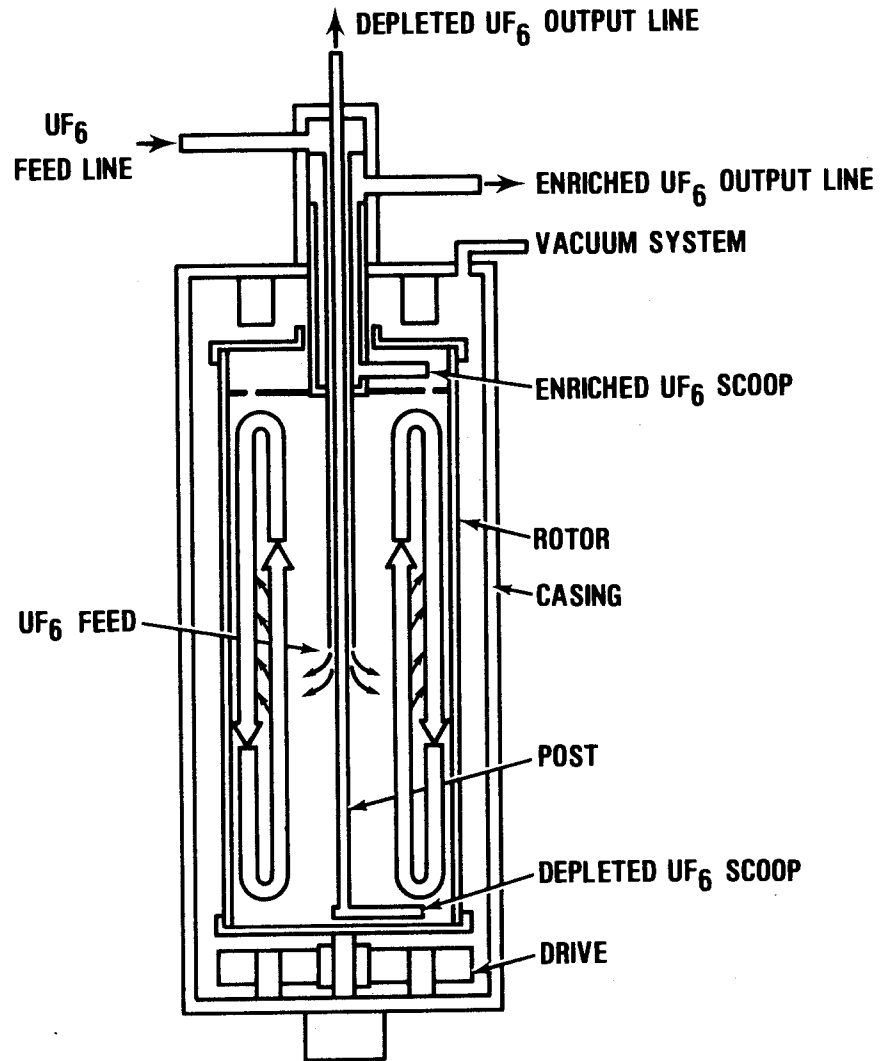


Fig. 1.1. Schematic of gas centrifuge.

2. ASSUMPTIONS

The method presented here assumes that the continuum equations for mass, momentum, and energy are sufficient to describe the flow. The conservation equations are written in cylindrical coordinates (r, θ, z) in the inertial frame with velocity components (u, v, w) . A further assumption is that all features can be averaged in the azimuthal (θ) direction and that thus the derivatives in the θ direction may be omitted. The flow is assumed to be laminar. The UF_6 gas is described using the ideal gas equation of state

$$P = \rho RT \quad (2.1)$$

with values for the properties C_p, γ, μ, κ , and ρD (D is the self-diffusivity of UF_6) which are constants for all points in the flow. Lastly, it is assumed that the changes in average molecular weight caused by the changes in concentration of small amounts of $^{235}UF_6$ (molecular weight 349) in a gas which is mostly $^{238}UF_6$ (MW 352) can be neglected. This allows the flow patterns to be calculated ignoring isotope separation and then the separation to be calculated as a final step.

The method is intended for calculating the steady-state behavior of a centrifuge. The solution scheme uses the steady-state assumption in a number of places as an aid to faster convergence so that in its present form it cannot simulate transient behavior accurately.



3. EQUATIONS OF MOTION

The equations of motion used in this paper are continuity:

$$\frac{\partial \rho}{\partial t} + \frac{1}{r} \frac{\partial}{\partial r} (\rho u r) + \frac{\partial}{\partial z} (\rho w) = \dot{\rho}_s \quad , \quad (3.1)$$

radial momentum:

$$\frac{\partial(\rho u)}{\partial t} = - \frac{\partial P}{\partial r} + \frac{\rho v^2}{r} + (\rho \dot{u})_s \quad , \quad (3.2)$$

axial momentum:

$$\frac{\partial(\rho w)}{\partial t} = - \frac{\partial P}{\partial z} + \frac{\mu}{r} \frac{\partial}{\partial r} \left(r \frac{\partial w}{\partial r} \right) + (\rho \dot{w})_s \quad , \quad (3.3)$$

angular momentum:

$$\frac{\partial(\rho v r)}{\partial t} + \frac{1}{r} \frac{\partial}{\partial r} (\rho u r v r) + \frac{\partial}{\partial z} (\rho w v r) = \frac{\mu}{r} \frac{\partial}{\partial r} \left[r^3 \frac{\partial}{\partial r} \left(\frac{v}{r} \right) \right] + (\rho \dot{v} r)_s \quad , \quad (3.4)$$

energy:

$$\begin{aligned} & \frac{\partial}{\partial t} [\rho (C_v T + \frac{1}{2} v^2)] + \frac{1}{r} \frac{\partial}{\partial r} [\rho u r (C_p T + \frac{1}{2} v^2)] + \frac{\partial}{\partial z} [\rho w (C_p T + \frac{1}{2} v^2)] \\ & = \frac{\kappa}{r} \frac{\partial}{\partial r} \left(r \frac{\partial T}{\partial r} \right) + \frac{\mu}{r} \frac{\partial}{\partial r} \left[r^2 v \frac{\partial}{\partial r} \left(\frac{v}{r} \right) \right] + \frac{\mu}{r} \frac{\partial}{\partial r} \left[r w \frac{\partial w}{\partial r} \right] \\ & + [\rho (C_p \dot{T} + \frac{1}{2} \dot{v}^2)]_s \quad . \end{aligned} \quad (3.5)$$

The above equations are all in divergence form except for radial momentum. The centrifugal force term in radial momentum cannot be converted to divergence form.

The equations of motion, Eqs. (3.1-3.5), represent Viecelli's approximations although he did not use the divergence form for his momentum

equations and used an internal energy equation for energy. There are many terms from the complete laminar equations which are missing in this approximation. The convection terms for both radial and axial momentum have been neglected, as well as most of the stress tensor from the three momentum equations and from the energy equation and the axial heat conduction from the energy equation. One of the theoretical advantages of a finite volume, finite difference, or finite element scheme is that the complete set of equations can be solved. Thus, a brief justification for the use of Viacelli's incomplete set may be in order. Adding terms to an equation set requires an increase in the size and complexity of the calculation and in the number of operations which must be done to get a solution. Further, terms whose overall contribution to the flow field is small may nevertheless change the character of the partial differential equations or of the difference equations so that achieving a solution may be more difficult than would be the case if they were neglected. Thus, there are strong disincentives which encourage the analyst to keep his equation set as simple as he can.

The separation chamber has boundaries at the top baffle, bottom cap, outer wall, and inner vacuum core. The boundary conditions at the outer wall ($r=a$) are

$$v = \Omega a , \quad (3.6)$$

where Ω is the rotation rate of the rotor and thus Ωa is the peripheral velocity, and

$$T = f(z) \quad (\text{a specified function}).$$

Those at the inner core are

$$u = 0 ,$$

$$\frac{\partial}{\partial r} \left(\frac{v}{r} \right) = 0 ,$$

$$\frac{\partial w}{\partial r} = 0 ,$$

$$\frac{\partial T}{\partial r} = 0 . \quad (3.7)$$

Those at the baffle and cap are

$$\frac{\partial u}{\partial z} = 0 \quad ,$$

$$w = 0 \text{ (except at baffle hole locations) } \quad ,$$

$$\frac{\partial v}{\partial z} = 0 \quad ,$$

$$\frac{\partial T}{\partial z} = 0 \quad . \quad (3.8)$$

At baffle hole locations, the axial mass flux ρw is specified.

Each of the equations of motion has a source term represented by a dot above and a subscript "s", e.g., $(\dot{\rho}u)_s$. The feed is introduced within the flow field as explicit sources of mass, momentum, and energy. These sources have a distribution in space that is determined by some theory which estimates the collisions of molecules in free molecular flow with the rotating gas. The rotating gas is, of course, described by the continuum equations. This subject will be discussed further in the next section. The scoop is simulated as a sink of mass, angular momentum, and energy located in the flow field. Because there are no convection terms for radial or axial momentum, it would be inconsistent to simulate sinks of these momentum components associated with the scoop mass sink. This subject will also be continued in the next section.

The isotope equation is described in the report by Park (ref. 4). The solution is obtained using the method described in that report. There is no need to repeat Park's discussions in this paper.



4. FINITE VOLUME EQUATIONS AND SOLUTION METHODS

The term "finite volume method" is fairly recent, but the ideas have been around for some time. Many engineers and scientists have seen the derivation of the partial differential equations for fluid flow from balances on control volumes as an exercise on the blackboard or in a textbook. Developing a discretization by reversing the process and integrating the p.d.e.'s over control volumes seems like too natural a step not to have occurred to many people independently. Patankar (ref. 5) wrote about the "Control Volume Formulation." The use of the conservation law form dates back at least as far as Lax (ref. 6). Roache (ref. 7) wrote earnestly about the need for the "conservative property" in finite difference equations. Patankar (ref. 5) made "consistency at control-volume faces" the first of his "Four Basic Rules."

The author regards any scheme which derives the set of discrete equations for the variables at nodes by dividing the region to be computed into a set of non-overlapping control volumes and integrating the partial differential equations over this set as a finite volume method. The author agrees wholeheartedly with Roache and Patankar about the necessity for consistent fluxes at the faces of the volumes. The author also accepts the preferability of using p.d.e.'s in the divergence or "conservation law" form following the reasons set forth by Lax.

A typical cell of the finite difference mesh is shown in Fig. 4.1. The half-cell offsets of radial and axial velocity (u and w) are arranged in this way in order to construct convective fluxes on the surfaces of the cell used to calculate mass and energy without having to average these velocities. The offset of angular velocity (v) is somewhat arbitrary. There are advantages to the offset position--principally the ability to construct the v^2 part of the centrifugal force term in radial momentum at a position halfway between adjacent pressures without having to average v . Probably, v could be defined at the same location as P and T and a difference algorithm constructed which would do as well as the one based upon the offset position.

The mesh is arranged so that the inner edge is located at $i=\frac{1}{2}$ and the outer edge at $i = NR+\frac{1}{2}$, where NR is the number of radial zones. The inner edge is not located at the center (i.e., $r_{\frac{1}{2}} > 0$). Rather, its location is usually determined by the equation

$$15 = \frac{(\Omega a)^2}{2 R T_0} \left[1 - \left(\frac{r_{\frac{1}{2}}}{a} \right)^2 \right], \quad (4.1)$$

where T_0 is a reference temperature. This is an expression for locating $r_{\frac{1}{2}}$ so that the density at $r_{\frac{1}{2}}$ under isothermal solid body rotation is e^{-15} times that at the $\frac{1}{2}$ wall. For convenience in defining boundary conditions, "image" cells are defined to the left (inside) of the inner edge and to the right (outside) of the wall. Similarly, the bottom cap is located at $j=\frac{1}{2}$ and the upper baffle at $j = NZ+\frac{1}{2}$ with image cells above and below these boundaries.

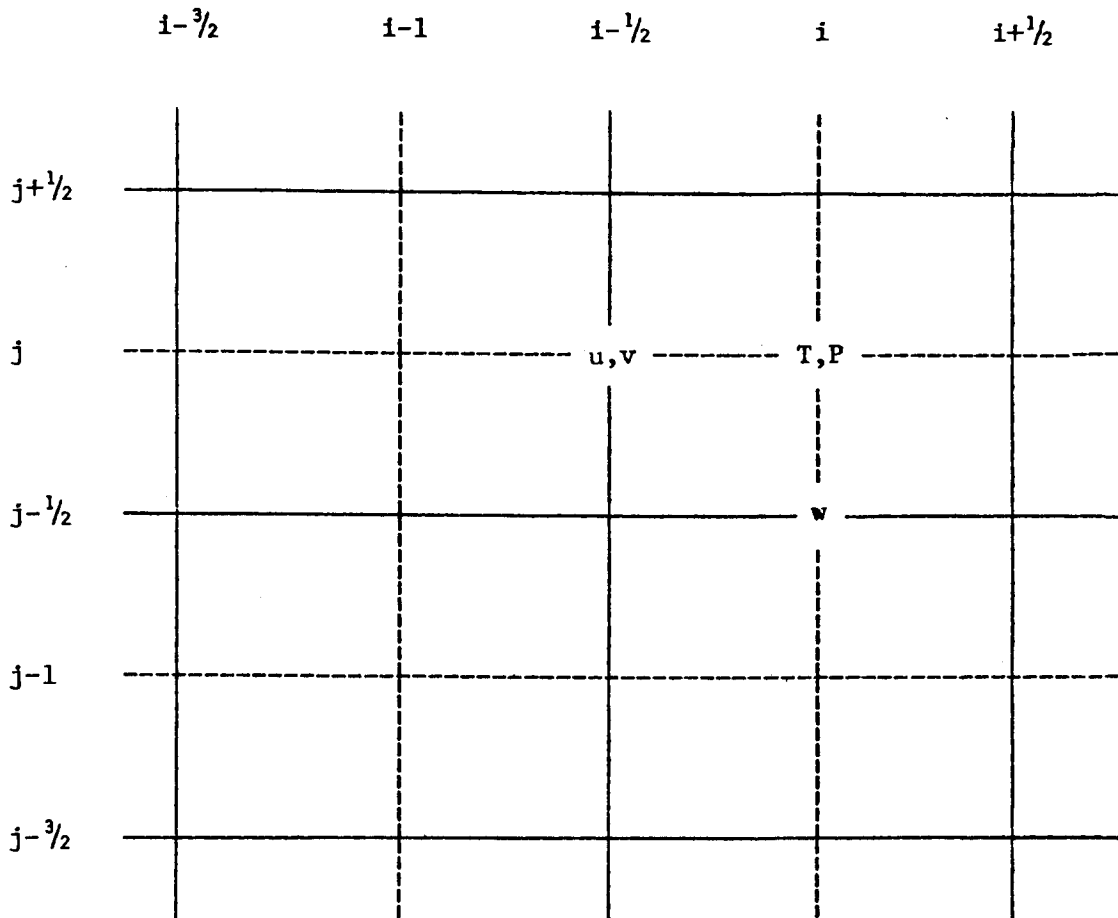


Fig. 4.1. Finite difference mesh.

A finite volume scheme requires definitions of the volumes. Also, some averaging operations require definition of surface areas. The control volume for mass and energy ($P_{i,j}$ and $T_{i,j}$) is $V_{i,j}$, which is defined by

$$V_{i,j} \equiv \pi (r_{i+\frac{1}{2}}^2 - r_{i-\frac{1}{2}}^2) (z_{j+\frac{1}{2}} - z_{j-\frac{1}{2}}) . \quad (4.2a)$$

The control volume for radial and angular momentum is

$$V_{i-\frac{1}{2},j} \equiv \pi (r_i^2 - r_{i-1}^2) (z_{j+\frac{1}{2}} - z_{j-\frac{1}{2}}) . \quad (4.2b)$$

The volume for axial momentum ($w_{i,j-\frac{1}{2}}$) is

$$V_{i,j-\frac{1}{2}} \equiv \pi (r_{i+\frac{1}{2}}^2 - r_{i-\frac{1}{2}}^2) (z_j - z_{j-1}) . \quad (4.2c)$$

For later use, some subvolumes must be defined, such as

$$V_{i-\frac{1}{4},j} \equiv \pi (r_i^2 - r_{i-\frac{1}{2}}^2) (z_{j+\frac{1}{2}} - z_{j-\frac{1}{2}}) , \quad (4.2d)$$

$$V_{i+\frac{1}{4},j} \equiv \pi (r_{i+\frac{1}{2}}^2 - r_i^2) (z_{j+\frac{1}{2}} - z_{j-\frac{1}{2}}) , \quad (4.2e)$$

$$V_{i,j-\frac{1}{4}} \equiv \pi (r_{i+\frac{1}{2}}^2 - r_{i-\frac{1}{2}}^2) (z_j - z_{j-\frac{1}{2}}) , \quad (4.2f)$$

etc.

In addition, some useful areas are

$$A_{i+\frac{1}{4}} \equiv \pi (r_{i+\frac{1}{2}}^2 - r_i^2) , \quad (4.2g)$$

$$A_{i-\frac{1}{2}} \equiv \pi (r_i^2 - r_{i-1}^2) , \quad (4.2h)$$

$$A_i \equiv \pi (r_{i+\frac{1}{2}}^2 - r_{i-\frac{1}{2}}^2) , \quad (4.2i)$$

etc.

Each of the five principal variables (P, T, u, w, v) has its own difference equation and its own solution scheme. The author has found it most convenient to discuss the solution of the finite volume difference equation for each of the principal variables immediately after the statement of the difference equation. However, the difference equations are derived from the p.d.e's through integration via finite volume methods and do not depend upon any specific solution scheme. The equation and solution for each of the principal variables will be described in turn.

4.1 RADIAL MOMENTUM

While the concept of integrating the p.d.e. to develop a difference equation for each cell is fairly straightforward, there may be some benefit in going through the process for at least one equation as a demonstration. The p.d.e. for radial momentum is given in Eq. (3.2). The integral of this equation over its appropriate control volume is

$$\int_{V_{i-\frac{1}{2},j}} \frac{\partial(\rho u)}{\partial t} dV = - \int_{V_{i-\frac{1}{2},j}} \frac{\partial P}{\partial r} dV + \int_{V_{i-\frac{1}{2},j}} \frac{1}{r} \rho v^2 dV$$

$$+ \int_{V_{i-\frac{1}{2},j}} (\rho u)_s dV .$$

Using the divergence theorem, the pressure gradient may be transformed to a surface integral. Making this transformation and letting $dV = 2\pi r dr dz$,

$$\begin{aligned}
 2\pi \int_{r_{i-1}}^{r_i} \int_{z_{j-\frac{1}{2}}}^{z_{j+\frac{1}{2}}} \frac{\partial(\rho u)}{\partial t} r dr dz &= -2\pi \int_{z_{j-\frac{1}{2}}}^{z_{j+\frac{1}{2}}} (P_i - P_{i-1}) r dz \\
 &+ 2\pi \int_{r_{i-1}}^{r_i} \int_{z_{j-\frac{1}{2}}}^{z_{j+\frac{1}{2}}} \frac{1}{r} \rho v^2 r dr dz \\
 &+ 2\pi \int_{r_{i-1}}^{r_i} \int_{z_{j-\frac{1}{2}}}^{z_{j+\frac{1}{2}}} (\dot{\rho u})_s r dr dz .
 \end{aligned}$$

At this point, average values of ρu , ρv^2 , and $(\dot{\rho u})_s$ over the volume $V_{i-\frac{1}{2},j}$ and average values of P_i and P_{i-1} between $z_{j-\frac{1}{2}}$ and $z_{j+\frac{1}{2}}$ are assumed to exist. In terms of these average values, the integrated equation becomes

$$\begin{aligned}
 \left. \frac{\partial(\rho u)}{\partial t} \right)_{i-\frac{1}{2},j} V_{i-\frac{1}{2},j} &= - (P_{i,j} - P_{i-1,j}) 2\pi \frac{r_i + r_{i-1}}{2} (z_{j+\frac{1}{2}} - z_{j-\frac{1}{2}}) \\
 &+ \rho v^2_{i-\frac{1}{2},j} 2\pi (r_i - r_{i-1}) (z_{j+\frac{1}{2}} - z_{j-\frac{1}{2}}) \\
 &+ (\dot{\rho u})_{s \ i-\frac{1}{2},j} V_{i-\frac{1}{2},j} .
 \end{aligned}$$

Approximate the time derivative by

$$\frac{\partial(\rho u)}{\partial t} \approx \frac{\rho u^{n+1} - \rho u^n}{\Delta t},$$

let

$$\rho_{i-\frac{1}{2},j} \approx \frac{P_{i,j} + P_{i-1,j}}{R(T_{i,j} + T_{i-1,j})},$$

and divide through by $V_{i-\frac{1}{2},j}$. The resulting finite volume equation for radial momentum at $i-\frac{1}{2},j$ is

$$\begin{aligned} \left. \frac{\rho u^{n+1} - \rho u^n}{\Delta t} \right)_{i-\frac{1}{2},j} &= - \frac{P_{i,j} - P_{i-1,j}}{r_i - r_{i-1}} + \frac{1}{r_{i-\frac{1}{2}}} \frac{(P_{i,j} + P_{i-1,j}) v_{i-\frac{1}{2},j}^2}{R(T_{i,j} + T_{i-1,j})} \\ &+ (\rho u)_{s \ i-\frac{1}{2},j}. \end{aligned} \quad (4.3)$$

The radial momentum difference equation is a simple explicit calculation. The values of P and T that are used are at whichever time level happens to be in memory when the operation is done (the algorithm does not require that both time levels n and $n+1$ be stored because the system is aimed at steady state). The boundary conditions on the wall and at the inner edge are accomplished by never changing the values at these locations.

4.2 AXIAL MOMENTUM

The difference equation for axial momentum at $i, j-\frac{1}{2}$ is

$$\begin{aligned} \left. \frac{\rho w^{n+1} - \rho w^n}{\Delta t} \right)_{i, j-\frac{1}{2}} &= - \frac{P_{i,j} - P_{i,j-1}}{z_j - z_{j-1}} + \frac{\mu}{r_i} \frac{1}{r_{i+\frac{1}{2}} - r_{i-\frac{1}{2}}} \\ &\quad \left\{ r_{i+\frac{1}{2}} \frac{w_{i+1, j-\frac{1}{2}}^{n+1} - w_{i, j-\frac{1}{2}}^{n+1}}{r_{i+1} - r_i} - r_{i-\frac{1}{2}} \frac{w_{i, j-\frac{1}{2}}^{n+1} - w_{i-1, j-\frac{1}{2}}^{n+1}}{r_i - r_{i-1}} \right\} \\ &\quad + (\rho w)_s \quad (4.4a) \end{aligned}$$

It is convenient to use ρ at whichever time level is in memory and thus have the difference equation cast as an equation for w instead of ρw . This is permissible because the system is only intended to calculate steady state. Density is not defined at $i, j-\frac{1}{2}$, but must be found by averaging, i.e.,

$$\rho_{i, j-\frac{1}{2}} = \frac{P_{i,j} + P_{i,j-1}}{R(T_{i,j} + T_{i,j-1})} \quad (4.4b)$$

The difference equation is solved using an implicit formulation in the radial direction. Terms multiplying the w 's at time level $n+1$ are collected on the LHS and all other terms on the RHS. Because there are no w terms for any value of j besides $j-\frac{1}{2}$, the rearranged difference equation becomes NZ tridiagonal sets of the form

$$A3_{i, j-\frac{1}{2}} w_{i+1, j-\frac{1}{2}}^{n+1} + A2_{i, j-\frac{1}{2}} w_{i, j-\frac{1}{2}}^{n+1} + A1_{i, j-\frac{1}{2}} w_{i-1, j-\frac{1}{2}}^{n+1} = B_{i, j-\frac{1}{2}} \quad (4.4c)$$

The boundary condition at the inner surface ($i=\frac{1}{2}$) is found by

$$w_{0, j-\frac{1}{2}}^{n+1} = w_{1, j-\frac{1}{2}}^{n+1} \quad (4.4d)$$

The boundary condition at the rotor wall ($i=NR+\frac{1}{2}$) is

$$w_{NR, j-\frac{1}{2}}^{n+1} = -w_{NR+1, j-\frac{1}{2}}^{n+1} \quad (4.4e)$$

The conditions on the caps ($j=\frac{1}{2}$, $j=NZ+\frac{1}{2}$) are that mass flux ρw is constant. These can be applied explicitly by calculating new values of w to meet this condition.

4.3 CONTINUITY (PRESSURE)

Although ρ is the correct variable for conservation of mass, continuity is expressed as an equation for P with the equation of state Eq. (2.1) providing the linkage between the two. One important part of Viacelli's solution scheme is the use of a steady-state continuity equation to calculate a pressure field for the next time step which will (ideally) produce a set of mass fluxes for that next time step which will exactly conserve mass. This approach is used in the ICE method (ref. 8).

Steady-state continuity is given by Eq. (3.1). The equation for mass conservation at time level $n+1$ may be written as:

$$0 = -\frac{1}{r} \frac{\partial}{\partial r} (r \rho u^n + \Delta t r \frac{\partial(\rho u)}{\partial t}) - \frac{\partial}{\partial z} (\rho w^n + \Delta t \frac{\partial(\rho w)}{\partial t}) + \dot{\rho}_s \quad (4.5a)$$

The mass flux derivatives are the same as the momentum derivatives and are given by Eqs. (3.2) and (3.3). Substituting these into Eq. (4.5a) and doing considerable rearranging, the continuity equation becomes an equation for pressure of the form:

$$\begin{aligned} 0 = & \frac{1}{r} \frac{\partial}{\partial r} \left(r \frac{\partial P^{n+1}}{\partial r} \right) + \frac{\partial}{\partial z} \left(\frac{\partial P^{n+1}}{\partial z} \right) - \frac{1}{r} \frac{\partial}{\partial r} \left(\frac{P^{n+1} v^2}{RT} \right) - \frac{\mu}{r} \frac{\partial}{\partial z} \left[\frac{\partial}{\partial r} \left(r \frac{\partial w}{\partial r} \right) \right] \\ & - \frac{1}{r} \frac{\partial}{\partial r} r (\rho u)_s - \frac{\partial}{\partial z} (\rho w)_s \\ & + \frac{1}{\Delta t} \left[-\frac{1}{r} \frac{\partial}{\partial r} r (\rho u)^n - \frac{\partial}{\partial z} (\rho w)^n + \dot{\rho}_s \right] \quad (4.5b) \end{aligned}$$

This is a linear p.d.e. in two space dimensions for the advanced time pressure field P^{n+1} . The term which is multiplied by $1/\Delta t$ represents the mass conservation error at time level n . It acts as a forcing function which drives the solution toward mass conservation. If it were absent, the solution to the equation would be a pressure field which would generate a mass flux field at level $n+1$ which would have the same distribution of mass conservation errors as the field at time level n .

The finite difference equation for $P_{i,j}^{n+1}$ is not derived by differencing the p.d.e. Eq. (4.5b), but rather by differencing the continuity equation, Eq. (4.5a), and then substituting from the differenced forms of

the radial and axial momentum equations. The difference equation for continuity based on finite volume concepts is

$$\begin{aligned}
0 = & -\frac{1}{r_i} \frac{1}{r_{i+\frac{1}{2}} - r_{i-\frac{1}{2}}} [\rho u]_{i+\frac{1}{2},j}^n r_{i+\frac{1}{2}} - \rho u]_{i-\frac{1}{2},j}^n r_{i-\frac{1}{2}} \\
& + \Delta t r_{i+\frac{1}{2}} \frac{\partial(\rho u)}{\partial t} \Big|_{i+\frac{1}{2},j} - \Delta t r_{i-\frac{1}{2}} \frac{\partial(\rho u)}{\partial t} \Big|_{i-\frac{1}{2},j} \\
& - \frac{1}{z_{j+\frac{1}{2}} - z_{j-\frac{1}{2}}} [\rho w]_{i,j+\frac{1}{2}}^n - \rho w]_{i,j-\frac{1}{2}}^n + \Delta t \frac{\partial(\rho w)}{\partial t} \Big|_{i,j+\frac{1}{2}} \\
& - \Delta t \frac{\partial(\rho w)}{\partial t} \Big|_{i,j-\frac{1}{2}} + \dot{\rho}_s \Big|_{i,j} . \tag{4.5c}
\end{aligned}$$

Equations (4.3) and (4.3a) approximate the time derivative terms. The final form of the difference equation is found by substituting these into Eq. (4.5c). It is

$$\begin{aligned}
0 = & \frac{1}{r_i} \frac{1}{r_{i+\frac{1}{2}} - r_{i-\frac{1}{2}}} \left\{ \rho u \right\}_{i+\frac{1}{2},j}^n r_{i+\frac{1}{2}} - r_{i+\frac{1}{2}} \frac{\Delta t}{r_{i+1} - r_i} (P_{i+1,j}^{n+1} - P_{i,j}^{n+1}) \\
& + \Delta t r_{i+\frac{1}{2}} \frac{P_{i+1,j}^{n+1} + P_{i,j}^{n+1}}{R (T_{i+1,j} + T_{i,j})} \frac{v_{i+\frac{1}{2},j}^2}{r_{i+\frac{1}{2}}} + \Delta t r_{i+\frac{1}{2}} (\dot{\rho} w)_s \Big|_{i+\frac{1}{2},j} \\
& - \left[\begin{array}{l} \text{four similar terms} \\ \text{centered at } i-\frac{1}{2},j \end{array} \right] \Big\} + \frac{1}{z_{j+\frac{1}{2}} - z_{j-\frac{1}{2}}} \left\{ \rho w \right\}_{i,j+\frac{1}{2}}^n \\
& + \frac{\Delta t}{z_{j+\frac{1}{2}} - z_{j-\frac{1}{2}}} (P_{i,j+1}^{n+1} - P_{i,j}^{n+1}) + \frac{\mu \Delta t}{r_i} \frac{\partial}{\partial r} \left(r \frac{\partial w}{\partial r} \right) \Big|_{i,j+\frac{1}{2}} \\
& + \Delta t (\dot{\rho} w)_s \Big|_{i,j+\frac{1}{2}} - \left[\begin{array}{l} \text{four similar terms} \\ \text{centered at } i,j-\frac{1}{2} \end{array} \right] \Big\} + \dot{\rho}_s \Big|_{i,j} . \tag{4.5d}
\end{aligned}$$

Boundary conditions come directly from the differenced momentum equations. All the boundaries have fixed values for mass flux. The conditions that lead to extrapolated values of pressure in the image cells outside the mesh are created using the appropriate momentum equation with the time rate of change set to zero. For instance, pressure in the image cell inside the mesh ($i=0$) is found from the radial momentum difference equation by

$$0 = \frac{\partial(\rho u)}{\partial t} \Big|_{\frac{1}{2},j} = - \frac{P_{1,j} - P_{0,j}}{r_1 - r_0} + \frac{1}{r_{\frac{1}{2}}} \frac{P_{1,j} + P_{0,j}}{R(T_{1,j} + T_{0,j})} v_{\frac{1}{2},j}^2 + (\dot{\rho}u)_s \Big|_{\frac{1}{2},j} \quad (4.5e)$$

The difference equation for pressure together with the boundary conditions lead to a set of simultaneous equations for P^{n+1} of the form

$$A_{i,j,1} P_{i,j-1}^{n+1} + A_{i,j,2} P_{i-1,j}^{n+1} + A_{i,j,3} P_{i,j}^{n+1} + A_{i,j,4} P_{i+1,j}^{n+1} + A_{i,j,5} P_{i,j+1}^{n+1} = B_{i,j} \quad (4.5f)$$

This set of equations has a matrix structure in which a square matrix with five non-zero diagonal stripes multiplies a vector of pressures to get the vector of right-hand sides. Viacelli solved the system exactly using Gaussian elimination. This solution used large amounts of computer time and required considerable computer memory for storage of scratch arrays. It was found that the successive line overrelaxation (SLOR) method could be used with large savings in both computer time and memory. Let superscript (ℓ) represent results from the ℓ th iteration of the SLOR method for a given time step. The $\ell+1$ th iteration is done by solving a tridiagonal system for each axial line which is derived by moving the axial terms from Eq. (4.5f) to the RHS; i.e.,

$$A_{i,j,2} P_{i-1,j}^{(\ell+1)} + A_{i,j,3} P_{i,j}^{(\ell+1)} + A_{i,j,4} P_{i+1,j}^{(\ell+1)} = B_{i,j} - A_{i,j,1} P_{i,j+1} - A_{i,j,5} P_{i,j-1} \quad (4.5g)$$

Note that the values of P on the RHS do not have an iteration level indicated. Satisfactory convergence can be obtained by using whichever level is resident in those locations at that moment which saves having to store two levels of pressure. The iteration is continued until satisfactory convergence is reached. The convergence criterion is

$$\max_{i,j} |P_{i,j}^{(\ell+1)} - P_{i,j}^{(\ell)}| / P_{WHL_i} < \epsilon \quad (4.5h)$$

where $PWHL_i$ is the pressure at r_i for wheel flow; and ϵ is a convergence constant which is typically 10^{-3} to 10^{-6} .

4.4 ANGULAR MOMENTUM

The difference equation for angular momentum at $i-\frac{1}{2}, j$ is

$$\begin{aligned}
 \frac{\partial(\rho vr)}{\partial t} \Big|_{i-\frac{1}{2}, j} \approx & - \frac{1}{r_{i-\frac{1}{2}}} \frac{1}{r_i - r_{i-1}} [(\rho ur)_{i,j} (vr)_{i,j} - (\rho ur)_{i-1,j} (vr)_{i-1,j}] \\
 & - \frac{1}{z_{j+\frac{1}{2}} - z_{j-\frac{1}{2}}} [(\rho w)_{i-\frac{1}{2}, j+\frac{1}{2}} (vr)_{i-\frac{1}{2}, j+\frac{1}{2}} \\
 & - (\rho w)_{i-\frac{1}{2}, j-\frac{1}{2}} (vr)_{i-\frac{1}{2}, j-\frac{1}{2}}] \\
 & + \frac{\mu}{r_{i-\frac{1}{2}}} \frac{1}{r_i - r_{i-1}} [r_i^3 \frac{1}{r_{i+\frac{1}{2}} - r_{i-\frac{1}{2}}} \left(\frac{v_{i+\frac{1}{2}, j}}{r_{i+\frac{1}{2}}} - \frac{v_{i-\frac{1}{2}, j}}{r_{i-\frac{1}{2}}} \right) \\
 & - r_{i-1}^3 \frac{1}{r_{i-\frac{1}{2}} - r_{i-\frac{3}{2}}} \left(\frac{v_{i-\frac{1}{2}, j}}{r_{i-\frac{1}{2}}} - \frac{v_{i-\frac{3}{2}, j}}{r_{i-\frac{3}{2}}} \right)] \\
 & + (\dot{\rho vr})_{s \ i-\frac{1}{2}, j} \quad . \quad (4.6a)
 \end{aligned}$$

Equation (4.6a) is not complete because ρur , ρw , and vr are not defined at the specified locations. The approximations for ρur and ρw are made in a way that ensures mass conservation for the control volume $V_{i-\frac{1}{2}, j}$. These are

$$\begin{aligned}
 (\rho ur)_{i,j} \approx & [(\rho ur)_{i+\frac{1}{2}, j} (r_i^2 - r_{i-\frac{1}{2}}^2) \\
 & + (\rho ur)_{i-\frac{1}{2}, j} (r_{i+\frac{1}{2}}^2 - r_i^2)] / (r_{i+\frac{1}{2}}^2 - r_{i-\frac{1}{2}}^2) \quad (4.6b)
 \end{aligned}$$

$$\begin{aligned}
 (\rho w)_{i, j-\frac{1}{2}} \approx & [(\rho w)_{i, j-\frac{1}{2}} (r_i^2 - r_{i-\frac{1}{2}}^2) \\
 & + (\rho w)_{i-1, j-\frac{1}{2}} (r_{i-\frac{1}{2}}^2 - r_{i-1}^2)] / (r_i^2 - r_{i-1}^2) \quad . \quad (4.6c)
 \end{aligned}$$

The averages for vr are

$$vr)_{i,j} \approx \frac{1}{2} [vr)_{i+\frac{1}{2},j} + vr)_{i-\frac{1}{2},j}] , \quad (4.6d)$$

$$vr)_{i-\frac{1}{2},j-\frac{1}{2}} \approx \frac{r_{i-\frac{1}{2}}}{2} [v_{i-\frac{1}{2},j} + v_{i-\frac{1}{2},j-1}] . \quad (4.6e)$$

The boundary conditions at the ends are accomplished by setting the image cell values to those for their neighbors in the interior cells. The angular velocity is actually defined at the outer wall ($i = NR + \frac{1}{2}$) so the nonslip condition is met by never changing v at $NR + \frac{1}{2}$. The inner boundary condition is a little more difficult. One of the desirable features of a conservative calculation is that quantities are conserved on the global scale represented by the total volume of the computing mesh as well as on a cell-by-cell basis. But the offset of the mesh used to calculate v compared to the mesh used to calculate mass and energy means that the total computing meshes for these variables do not coincide. The decision was made to treat $r_{\frac{1}{2}}$ as the "true" boundary for all variables. This requires a boundary condition at the inner edge which is

$$\frac{v_{-\frac{1}{2},j}}{r_{-\frac{1}{2}}} = \frac{v_{+\frac{3}{2},j}}{r_{+\frac{3}{2}}} . \quad (4.6f)$$

Viecelli proposed solving the angular momentum equation in a steady-state form as an aid to improved convergence. He also proposed that the system of simultaneous equations which results from Eqs. (4.6a-4.6f) should be solved by SLOR, but with only one iteration per time step. The result is almost identical to that used for pressure, i.e.,

$$A_{i,j,2} v_{i+\frac{1}{2},j}^{n+1} + A_{i,j,3} v_{i-\frac{1}{2},j}^{n+1} + A_{i,j,4} v_{i-\frac{3}{2},j}^{n+1} = B_{i,j} - A_{i,j,1} v_{i-\frac{1}{2},j+1} - A_{i,j,5} v_{i-\frac{1}{2},j-1} . \quad (4.6g)$$

As was the case with pressure, the values of v on the RHS are at whichever time level happens to be in memory at that moment. There is a feedback loop between the pressure and angular momentum equations which occurs because the value of v^2 strongly influences the radial pressure difference which, in turn, controls changes in the radial velocity field which lead to changes in v . The existence of this loop has forced underrelaxation of the angular momentum step for some problems.

4.5 ENERGY

The difference equation for energy at i, j is

$$\begin{aligned}
 & \frac{\rho(C_v T + \frac{1}{2}v^2)_{i,j}^{n+1} - \rho(C_v T + \frac{1}{2}v^2)_{i,j}^n}{\Delta t_e} = \frac{1}{\bar{r}_i} \frac{1}{r_{i+\frac{1}{2}} - r_{i-\frac{1}{2}}} [\rho w]_{i+\frac{1}{2},j} \\
 & (C_p T_{i+\frac{1}{2},j}^{n+1} + \frac{1}{2}v_{i+\frac{1}{2},j}^2) - \rho w]_{i-\frac{1}{2},j} (C_p T_{i-\frac{1}{2},j}^{n+1} + \frac{1}{2}v_{i-\frac{1}{2},j}^2) \\
 & - \frac{1}{z_{j+\frac{1}{2}} - z_{j-\frac{1}{2}}} \{ [\rho w (C_p T^{n+1} + \frac{1}{2}v^2)]_{i,j+\frac{1}{2}} \\
 & - [\rho w (C_p T^{n+1} + \frac{1}{2}v^2)]_{i,j-\frac{1}{2}} \} \\
 & + \frac{\kappa}{\bar{r}_i} \frac{1}{r_{i+\frac{1}{2}} - r_{i-\frac{1}{2}}} [r_{i+\frac{1}{2}} \frac{T_{i+1,j}^{n+1} - T_{i,j}^{n+1}}{r_{i+1} - r_i} - r_{i-\frac{1}{2}} \frac{T_{i,j}^{n+1} - T_{i-1,j}^{n+1}}{r_i - r_{i-1}}] \\
 & + \frac{\mu}{\bar{r}_i} \frac{1}{r_{i+\frac{1}{2}} - r_{i-\frac{1}{2}}} [\frac{r_{i+\frac{1}{2}}^2 v_{i+\frac{1}{2},j}}{r_{i+1} - r_i} (\frac{v}{r})_{i+1,j} - \frac{v}{r}]_{i,j} \\
 & - \frac{r_{i-\frac{1}{2}}^2 v_{i-\frac{1}{2},j}}{r_i - r_{i-1}} (\frac{v}{r})_{i,j} - \frac{v}{r}]_{i-1,j}) \\
 & + \frac{\mu}{\bar{r}_i} \frac{1}{r_{i+\frac{1}{2}} - r_{i-\frac{1}{2}}} [r w \frac{\partial w}{\partial r}]_{i+\frac{1}{2},j} - r w \frac{\partial w}{\partial r}]_{i-\frac{1}{2},j} \\
 & + [\rho(C_p \dot{T} + \frac{1}{2}v^2)]_{s i,j} .
 \end{aligned} \tag{4.7a}$$

Many of the terms in this equation need to be defined. The approximations are as follows:

$$T_{i+\frac{1}{2},j} \approx \frac{1}{2}(T_{i+1,j} + T_{i,j}), \quad (4.7b)$$

$$v_{i,j}^2 \approx [v_{i+\frac{1}{2},j}^2 (r_{i+\frac{1}{2}}^2 - r_i^2) + v_{i-\frac{1}{2},j}^2 (r_i^2 - r_{i-\frac{1}{2}}^2)] / (r_{i+\frac{1}{2}}^2 - r_{i-\frac{1}{2}}^2), \quad (4.7c)$$

$$\begin{aligned} [\rho_w C_p T]_{i,j+\frac{1}{2}} &\approx \frac{1}{2} C_p [(T_{i,j+1} + T_{i,j}) \rho_w]_{i,j+\frac{1}{2}} \\ &\quad - \alpha (T_{i,j+1} - T_{i,j}) |\rho_w|_{i,j+\frac{1}{2}}, \end{aligned} \quad (4.7d)$$

$$\begin{aligned} [\rho_w \frac{1}{2} v^2]_{i,j+\frac{1}{2}} &\approx \frac{1}{4} [(v_{i,j+1}^2 + v_{i,j}^2) \rho_w]_{i,j+\frac{1}{2}} \\ &\quad - \alpha (v_{i,j+1}^2 - v_{i,j}^2) |\rho_w|_{i,j+\frac{1}{2}}, \end{aligned} \quad (4.7e)$$

$$\left(\frac{v}{r}\right)_{i,j} \approx \frac{1}{2} \left(\frac{v_{i+\frac{1}{2},j}}{r_{i+\frac{1}{2}}} + \frac{v_{i-\frac{1}{2},j}}{r_{i-\frac{1}{2}}} \right). \quad (4.7f)$$

$$\begin{aligned} r w \frac{\partial w}{\partial r} \Big|_{i+\frac{1}{2},j} &\approx \frac{1}{2} \frac{r_{i+\frac{1}{2}}}{r_{i+1} - r_i} \{ (w_{i+1,j+\frac{1}{2}} + w_{i,j+\frac{1}{2}}) \\ &\quad (w_{i+1,j+\frac{1}{2}} - w_{i,j+\frac{1}{2}}) (z_{j+\frac{1}{2}} - z_j) + (w_{i+1,j-\frac{1}{2}} + w_{i,j-\frac{1}{2}}) \\ &\quad (w_{i+1,j-\frac{1}{2}} - w_{i,j-\frac{1}{2}}) (z_j - z_{j-\frac{1}{2}}) \} / (z_{j+\frac{1}{2}} - z_{j-\frac{1}{2}}). \end{aligned} \quad (4.7g)$$

Viecelli used the weighted donor cell differencing for the axial heat flux as shown in Eq. (4.7d). He also used a separate time step for energy Δt_e . This is usually 100 times the regular time step. The donor cell factor α is found by searching the mesh for a minimum axial cell transit time given by

$$\min_{i,j} \left| \frac{z_{j+1} - z_j}{w_{i,j+\frac{1}{2}}} \right|,$$

and then dividing this into Δt_e . This quotient multiplied by a safety factor of about 1.2 is used for α . If this value is larger than 1.0, Δt_e must be lowered until $\alpha < 1.0$. The boundary conditions at the caps are accomplished by simply setting the values of T in the image cells to those of their neighbors in the interior. The inner boundary condition is the same; i.e.,

$$T_{0,j} = T_{1,j} \quad (4.7h)$$

The wall boundary condition is satisfied by a linear extrapolation to the image cell of the form

$$\frac{T_{NR+1,j} - TW_j}{r_{NR+1} - r_{NR+1/2}} = \frac{T_{NR+1,j} - T_{NR,j}}{r_{NR+1} - r_{NR}} \quad (4.7i)$$

where TW_j is the temperature of the wall at z_j .

Because the algorithm is only intended for steady state, it is not necessary that the rate of change in energy accurately take into account changes in either density or kinetic energy. Thus, it is possible to reduce the LHS of Eq. (4.7a) to

$$\frac{\partial}{\partial t} [\rho(C_v T + \frac{1}{2}v^2)]_{i,j} \approx \frac{\rho_{i,j}^n}{\Delta t_e} (T_{i,j}^{n+1} - T_{i,j}^n) \quad (4.7j)$$

The set of simultaneous equations that results from Eq. (4.7a-4.7j) can be written as

$$\begin{aligned} A_{i,j,1} T_{i,j+1}^{n+1} + A_{i,j,2} T_{i+1,j}^{n+1} + A_{i,j,3} T_{i,j}^{n+1} + A_{i,j,4} T_{i-1,j}^{n+1} \\ + A_{i,j,5} T_{i,j-1}^{n+1} = B_{i,j} \end{aligned} \quad (4.7k)$$

Viecelli solved his energy equation with SLOR. It has been found from experiment that stability requires that all of the axial donor cell terms must appear at the same time level so that, for an SLOR formulation, part of the central diagonal term, $A_{i,j,3}$, must be placed on the RHS. The SLOR equation is

$$A_{i,j,2} T_{i+1,j}^{n+1} + A'_{i,j,3} T_{i,j}^{n+1} + A_{i,j,4} T_{i-1,j}^{n+1} = B_{i,j} - A''_{i,j,3} T_{i,j}^n - A_{i,j,1} T_{i,j+1}^n - A_{i,j,5} T_{i,j-1}^n, \quad (4.71)$$

where

$$A''_{i,j,3} = -\alpha \frac{C_p}{2} \frac{1}{z_{j+\frac{1}{2}} - z_{j-\frac{1}{2}}} [|\rho w|_{i,j+\frac{1}{2}} + |\rho w|_{i,j-\frac{1}{2}}]; \quad (4.7m)$$

and $A'_{i,j,3}$ contains the rest of $A_{i,j,3}$. As in angular momentum, the energy equation is not iterated but is solved only once for each time step.

4.6 SOURCE AND SINK TERMS

As was mentioned in the previous section, the feed and the interaction of the gas with the tails scoop lead to source terms in mass, angular momentum, and energy. In practice, source terms in radial and axial momentum are neglected. The conservative finite volume approach makes calculation of the sources particularly easy. For mass, the source is simply the amount of mass arriving within a control volume per unit time divided by the volume. Similarly, the angular momentum source is the mass rate multiplied by the angular velocity of the arriving molecules and the radius of the interaction, again divided by the volume. For feed, the average angular velocity is zero. For energy, the source is the mass rate times the total enthalpy $C_p T + \frac{1}{2} (u^2 + v^2 + w^2)$ of the molecules divided by the volume.

Although the principles are the same, the correct treatment of the scoop is more complicated. The control volume which contains the cell must have explicit sinks of mass, angular momentum, and energy. The mass sink is obvious. The angular momentum sink, thanks to Newton's Third Law, is exactly equal to the torque applied to the arm that holds the scoop divided by the volume. As Olander mentioned, the gas which flows past the scoop is heated by the interaction. However, the scoop is not moving in the laboratory frame so that it cannot be an explicit source of energy. The mass sink aspect of the scoop leads to an energy sink whose magnitude is the mass sink rate multiplied by the stagnation enthalpy divided by the volume. The heating near the scoop is automatically calculated by the shear terms and the transformation of kinetic to internal energy which are integral parts of the energy equation.

4.7 ORDER OF EQUATIONS IN SOLUTION

A single time step consists of an iteration of the angular momentum equation followed by an iteration of the energy equation, several iterations of the pressure equation (after 50-200 time steps, the initial pseudo-transient will die away, and the number of pressure iterations per time step will usually fall to between 1 and 5), and fresh solutions of the radial and axial momentum equations. This order of operations is not mandatory although the sequence [pressure--radial (or axial) momentum--axial (or radial) momentum] gives the closest to a mass conserving flow field for use by the angular momentum and energy equations.



5. STABILITY AND LIMITATIONS OF THE METHOD

The SLOR solutions specified for all of the governing equations except radial momentum calculate radial transport implicitly. Consequently, radial stability limitations should be mild. The axial transport of angular momentum and energy is, in effect, explicit. Thus, one might expect Courant limits in the axial direction. An attempted stability analysis of the solution scheme did not yield any useful results. The system seems to have a time step limit of the form

$$\Delta t < .008 \min_{i,j} \left| \frac{\Delta z}{w} \right| . \quad (5.1)$$

This limit is both very crude and highly empirical, but it is useful for order of magnitude estimates.

In the discussion of the angular momentum equation in the previous section, it was noted that stability required an underrelaxation of the angular momentum equation. In addition, it has been found to be advisable that the relaxation factor be further limited so that no value of angular velocity may change by more than 1% in any time step. This can be a temporary limit that acts during the first 50-200 time steps during which the changes in the system variables are fairly vigorous. After these initial transients have decayed, the relaxation factor may be increased to its "stable" limit.

The Viacelli approximations neglect axial shear stresses and axial heat conduction. The end cap boundary conditions are free-slip and adiabatic which are consistent with the absence of axial diffusion of momentum and energy. These boundary conditions preclude development of the "Ekman" boundary layers which are assumed to exist on the caps (refs. 9,10). There have been discussions of this lack among the author and numerous colleagues, and some effort has been made toward remedying it. To date, no model of the Ekman layers has been developed which is satisfactory for the finite volume approach as outlined in this paper so that the lack of Ekman layers remains a notable omission.



6. RESULTS

A test case has been run using machine parameters which were published by Wood and Sanders (ref. 11). This case represents the optimum parameters from Table 2 of ref. 11. Figure 6.1 is a plot of the streamlines. Reference 11 contains plots of streamlines for a linear wall temperature (Fig. 8) and a scoop (Fig. 9). These two plots are reproduced in Figs. 6.2a and 6.2b. Unfortunately, ref. 11 does not show a streamline plot for a combined case. The optimum quoted in Table 2 of ref. 11 was found by linear superposition of the scoop and linear wall temperature solutions together with some mass feed solutions. Thus, a plot of the streamlines for the combined case would have features from both Figs. 8 and 9, ref. 11 (i.e., Figs. 6.2a and 6.2b, respectively).

Figure 6.1 shows some of the qualitative features that one might ascribe to a plot of streamlines from the ref. 11 optimum case by mentally combining Figs. 6.2a and 6.2b. A cell which is centered at about one-half scale height radially and one-half the rotor length axially looks like the cell shown in Fig. 6.2a. Similarly, Fig. 6.1 contains a cell centered at about four scale heights radially and near the bottom axially which resembles the cell shown in Fig. 6.2b. The differences in the shape of the streamlines for this cell at the bottom may be partially explained by the inclusion of an Ekman layer model and a much finer axial resolution in the calculations of ref. 11 compared to those which are plotted in Fig. 6.1. Such deviations in the fine structure are not surprising. Nevertheless, one may conclude that the test calculation for this paper produces streamlines similar to those from the same case calculated using the methods of ref. 11.

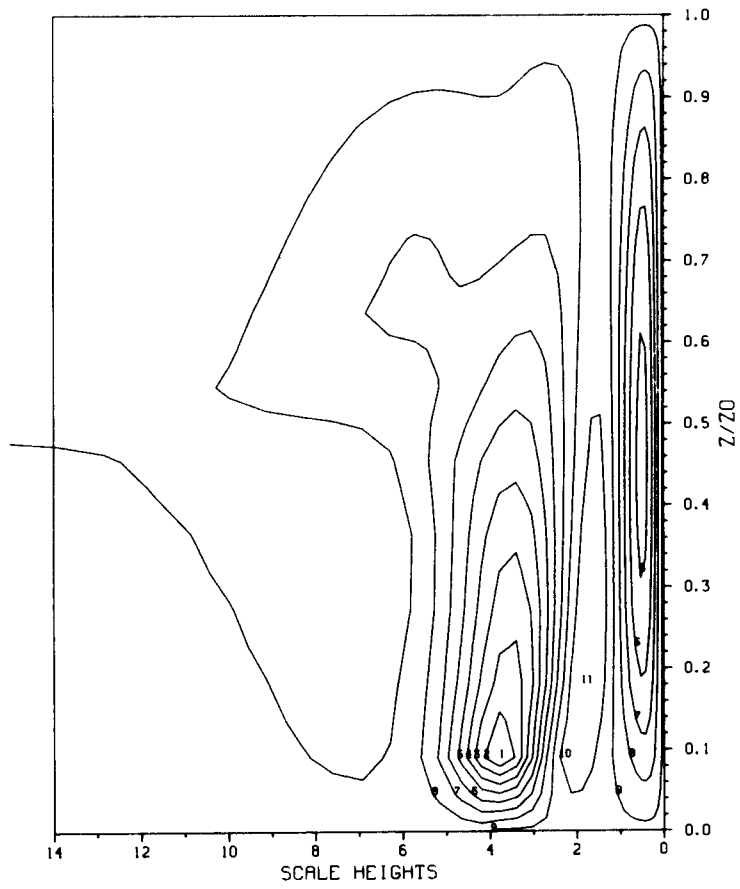


Fig. 6.1. Streamlines for test case.

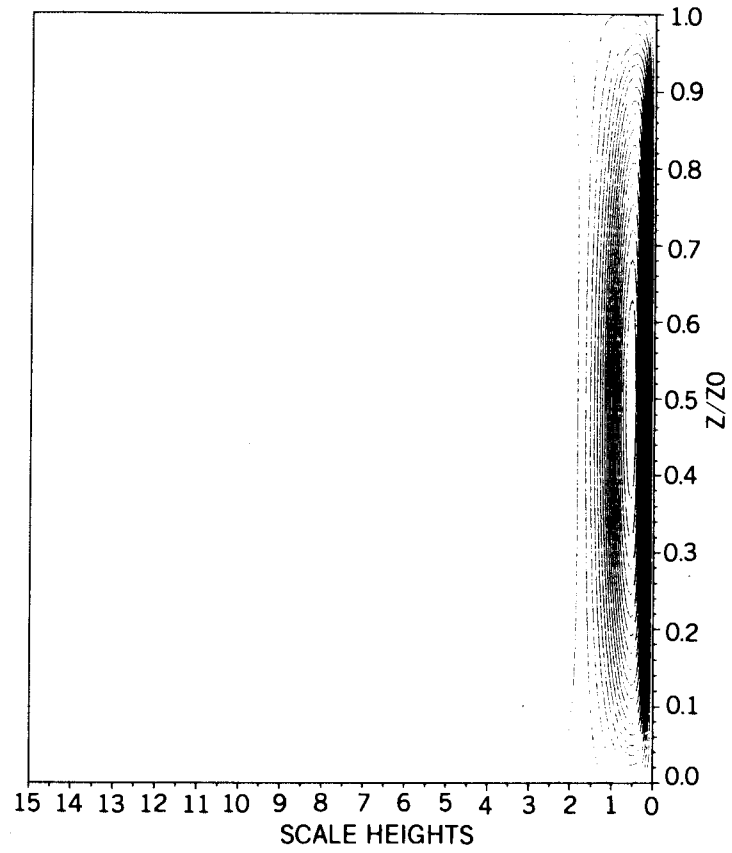


Fig. 6.2a. Streamline plot for "linear wall temperature drive"
(Source: reproduced from Fig. 8 of ref. 11).

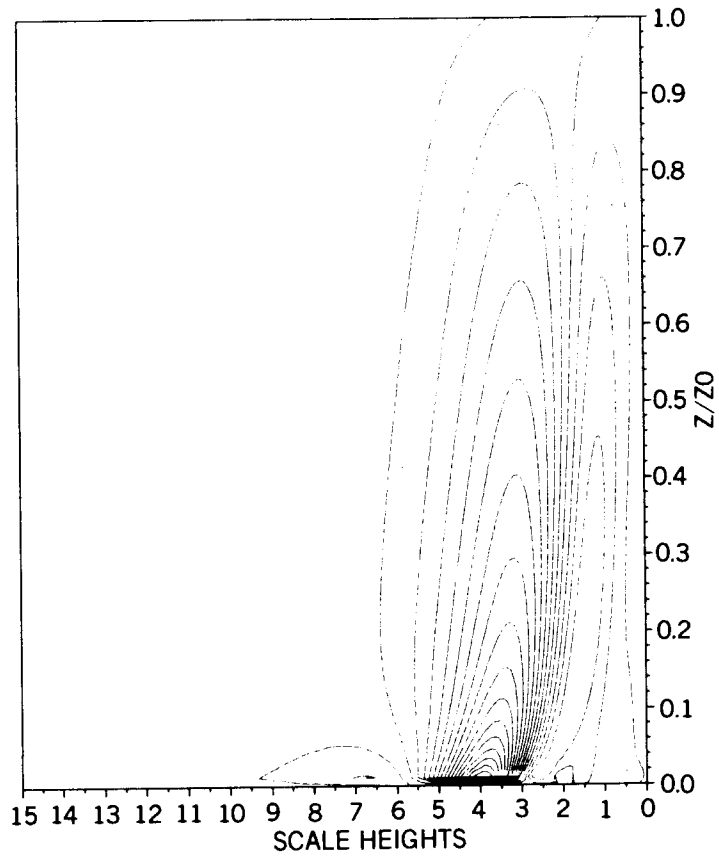


Fig. 6.2b. Streamline plot for "scoop drive"
(Source: reproduced from Fig. 9 of ref. 11).

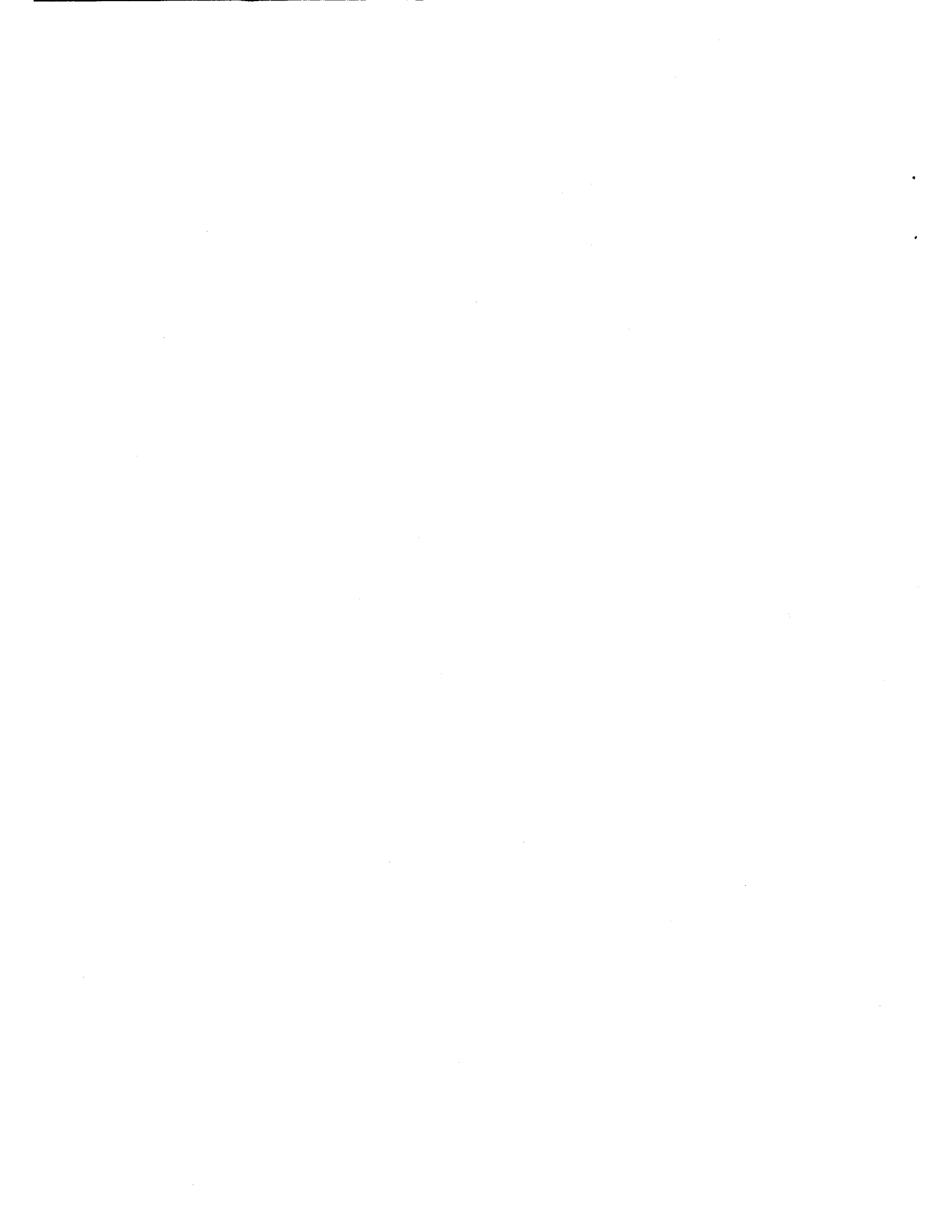
ACKNOWLEDGMENTS

The work described in this paper was funded by the United States Department of Energy through contract No. W-7405-eng-26 with Union Carbide Corporation Nuclear Division. The contract for operating the Oak Ridge complex was assumed by Martin Marietta Energy Systems, Inc., in April 1984. The primary sponsor for the project is E. von Halle (Operations Analysis and Planning Division). Some portions were also sponsored by H. G. Wood, III, and others by A. J. Szady, Jr. (both of Separation Systems Division). Over the years, the author has had many enlightening discussions with these gentlemen as well as with G. Sanders and J. E. Park.



REFERENCES

1. D. R. Olander, "The Gas Centrifuge", Scientific American, 239, (2) (August 1978).
2. E. von Halle, The Countercurrent Gas Centrifuge for the Enrichment of U-235, K/OA-4058, Union Carbide Corporation, Nuclear Division, Oak Ridge Gaseous Diffusion Plant, November 1977.
3. R. L. Hoglund, J. Shacter, and E. Von Halle, Encyclopedia of Chemical Technology, John Wiley & Sons, New York, 1979, s.v. "Diffusion Separation Methods".
4. J. E. Park, Calculation of the Isotope Distribution in a Gas Centrifuge, K/CSD/TM-36, Union Carbide Corporation, Nuclear Division, Oak Ridge Gaseous Diffusion Plant, February 1981.
5. S. V. Patankar, Numerical Heat Transfer and Fluid Flow, McGraw-Hill, New York, 1980.
6. P. D. Lax, "Weak Solutions of Nonlinear Hyperbolic Equations and their Numerical Computation", Communication on Pure and Applied Mathematics, 7, (1), 159-193, (1954).
7. P. J. Roache, Computational Fluid Dynamics, Hermosa Publishers, Albuquerque, New Mexico, 1972.
8. C. W. Hirt et al., "An Arbitrary Lagrangian - Eulerian Computing Method for All Flow Speeds", J. of Computational Physics, 14, 227-253 (1974).
9. H. G. Wood III and J. B. Morton, "Onsager's Approximation for the Fluid Dynamics of a Gas Centrifuge", J. of Fluid Mechanics, 101, (1), 1-31 (1980).
10. G. F. Carrier, "Phenomena in Rotating Fluids", presented at the Eleventh International Congress of Applied Mechanics, Munich, Germany, 1964.
11. H. G. Wood III and G. Sanders, An Analysis of the Effect of the Flow Field on the Separative Performance of a Gas Centrifuge K/Ts-10435, Union Carbide Corporation, Nuclear Division, Oak Ridge Gaseous Diffusion Plant, June 1981.



DISTRIBUTION

1. J. S. Crowell
2. M. G. Culbertson
- 3-12. J. R. Kirkpatrick
13. R. P. Leinius/G. E. Whitesides/
Enrichment Technology Library
- 14-16. A. S. Quist
17. A. J. Szady, Jr.
18. J. N. Tunstall
19. E. von Halle
- 20-21. Enrichment Technology Library
- 22-51. Office of Scientific and Technical Information
52. ORGDP Plant Records, RC